

Tactile Gesture Recognition with Built-in Joint Sensors for Industrial Robots

Deqing Song^{1*}, Weimin Yang^{1*}, Maryam Rezaayati^{1,2†}, Hans Wernher van de Venn^{2†}

Abstract—While gesture recognition using vision or robot skins is an active research area in Human-Robot Collaboration (HRC), this paper explores deep learning methods relying solely on a robot’s built-in joint sensors, eliminating the need for external sensors. We evaluated various convolutional neural network (CNN) architectures and collected two datasets to study the impact of data representation and model architecture on the recognition accuracy. Our results show that spectrogram-based representations significantly improve accuracy, while model architecture plays a smaller role. We also tested generalization to new robot poses, where spectrogram-based models performed better. Implemented on a Franka Emika Research robot, two of our methods, STFT2DCNN and STT3DCNN, achieved over 95% accuracy in contact detection and gesture classification. These findings demonstrate the feasibility of external-sensor-free tactile recognition and promote further research toward cost-effective, scalable solutions for HRC.

I. INTRODUCTION

Transiting from Industry 4.0 to Industry 5.0, the industry is putting more emphasis on placing the well-being of the industry workers at the center of the production process [1], [2], [3]. When humans have control over tasks, they tend to feel more comfortable when they can influence the robot’s movements [4]. As a result, numerous studies focus on the effects of various communication forms in collaborative systems, particularly highlighting the high ratings for gesture and touch [5]. Tactile perception has primarily relied on artificial skins embedded with sensors that detect touch, pressure, and other physical interactions. There are generally two types of artificial skins according to the sensor type and how their sensor data feed into machine learning algorithms [6]: general tactile sensors producing continuous (analog) signals [7] and neuromorphic devices providing spike-based signals in a manner akin to biological skin. The first type faces practical limitations as the number and resolution of tactile sensors increase, leading to large amounts of tactile data that strain communication bandwidth and computational resources [8]. To these limitations, event-based spike signals—mirroring human neural systems—has been introduced [9]. Although spike-signal-based skins mitigate

certain limitations of analog alternatives, both categories of artificial skins face the following challenges:

- The artificial skin system often comprises numerous miniature components, increasing design, operation, and maintenance complexity [10], [11], [12].
- The Artificial skin system is an external solution, requiring either the purchase of an entirely new robot or a separate skin system and its integration [13], [14], [15].

This leads to the difficulty in deploying those kind of systems in existing large-scale manufacturing scenarios. Hence, artificial skin systems may not always be the ideal approach for certain collaborative applications. To circumvent these limitations, researchers increasingly consider alternative tactile recognition methods that exploit robots’ inherent sensing capabilities—for example, the advanced torque sensors and internal parameters built into many modern robots. Such built-in feedback can deliver valuable real-time information about robot–environment interactions, all without additional hardware. While these approaches significantly reduce system complexity and data-transfer requirements, the majority of joint-torque-based studies has focused on collision detection rather than identifying and classifying multiple human touch gestures.

A. The Paper’s Contribution

Motivated by the aforementioned gap, this paper investigates the potential of relying solely on the robot’s built-in joint sensors for tactile gesture recognition tasks. Concretely, we make the following contributions:

- We demonstrate the feasibility of recognizing multiple tactile gestures on a robot solely by using internal joint sensor data, eliminating the need for expensive and complex external tactile sensors.
- We introduce a tactile gesture recognition framework that combines spectrogram-based transformations of internal joint sensor data with CNN-based classification, effectively bridging the gap between time-domain signal processing and image-based deep learning.
- We conduct a comprehensive exploration of signal representations and implement a variety of strategies to capture the distinct signal patterns generated by tactile gestures.
- We compare and evaluate the performance of these methods in real-time on a Franka Emika Research robotic platform, validating their practical applicability.
- To ensure the reproducibility and facilitate further research, we have made our complete dataset and source

Authors indicated by ¹ are with Dep. of Informatics, University of Zurich Switzerland. `FirstName.LastName@uzh.ch`

Authors indicated by ² are with the Institute of Mechatronics systems, Zurich University of Applied Science, Switzerland. `FirstName.LastName@zhaw.ch`

Authors marked with * contributed equally and marked with † are corresponding authors. This work was supported by the Eurostars project (Grant No. E!3087) titled *SmartSenseAI*. The authors would like to thank generative AI models (ChatGPT and Gemini) for assisting with improving the clarity of the manuscript.

The code and dataset corresponding to this work is provided at <https://github.com/MindLabZHAW/tactileGestureDetection>

code publicly available.

II. RELATED WORK

A. Collision Detection

Lee et al. [13] integrated the robot’s dynamic model with its friction model to monitor accelerations, whereas Ren et al. [16] introduced an extended state observer to estimate external torque. Zurlo et al. [17] proposed an observer that tracks energy and generalized momentum before applying a Contact Particle Filter algorithm. These model-based methods can be highly sensitive to motor noise and often require extensive system modeling and threshold tuning. Consequently, researchers have begun to explore approaches that partly or entirely remove the need for explicit dynamic models, thereby simplifying detection systems.

To eliminate explicit dynamic modeling and complex inverse dynamic computations, Sharkawy et al. employed a simple MIMO neural network [18] in place of explicit modeling. In subsequent work, they compared different neural network structures—MLFFNN, CFNN, and RNN—for estimating external torque and detecting collisions [19]. Among these, the MLFFNN with a single hidden layer achieved the best overall performance, exhibiting the lowest approximation error, mean squared error (MSE), collision threshold, and collision detection time, but it requires intrinsic torque sensors. By contrast, the MLFFNN with two hidden layers, the CFNN, and the RNN also achieved acceptable performance without intrinsic torque information, making them applicable to a wider range of robots. Aiming to avoid manual threshold tuning, Park et al. presented a supervised collision detection algorithm that combines a traditional Momentum Observer (MO) with a 1D-CNN and an SVM [20]. They later extended this framework to incorporate One-Class SVM and Auto-encoders for unsupervised collision interpretation [21]. Building on a vibration model, Min et al. [22] employed three BP-ANNs for collision interpretation. Although Min et al. [22] used an external accelerometer, we consider their approach external-sensor-free for modern collaborative robots (cobots), which typically have joint sensors capable of measuring acceleration. Leveraging the full suite of modern cobots’ joint-sensor data (such as external torques and accelerations), Heo et al. [12] developed CollisionNet, a modified Auto Regressive (AR) network that uses convolution operations. This approach takes raw sensor outputs as inputs and directly generates a collision prediction signal, avoiding both explicit modeling and threshold tuning. Czubenko et al. [23] also employed neural networks, including AR, RNN, CNN-LSTM, and a mixed convolutional LSTM (MC-LSTM), for collision detection, where their experiments showed that using ConvLSTM neurons is particularly effective for modeling robot dynamics. Kim et al. [24] introduced a Versatile Modularized Neural Network (MNN), primarily focused on reducing retraining overhead when transitioning between different cobots.

B. Extended classification and tactile recognition

Beyond collision detection, researchers have also examined collision classification [22]. For example, Min et al. [22] distinguished between no-contact scenarios and collisions at two points in three directions, while Amin et al. [25] used a 1D-CNN to classify no-contact conditions alongside intentional and incidental contact on two distinct links.

Similarly, in the realm of tactile gesture recognition, which deals with active contact events, the cobot must first detect the contact, then identify which gesture is applied. Bianchini et al. [26] defined four types of gestures — Tap (e.g., hit, pat, poke, slap), Touch (e.g., contact, lift, press), Grab (e.g., cradle, pinch, squeeze), and Slip (e.g., rub, scratch, stroke) — and evaluated several classification approaches, including traditional machine learning methods (Decision Trees, SVMs), and a 1D CNN network. Their experiments, conducted on a UR5e cobot equipped with the internal six-axis wrist force-torque sensor, demonstrated that the neural network classifier achieved the best performance, with a test accuracy of 81%. Our work builds upon this foundation by investigating a specific deep learning approach. We further investigate CNN-based deep learning methods on various 3D data representations (including spectrograms), and provide a detailed analysis of how input representations and network architectures influence performance, particularly under domain shifts across unseen robot poses, a crucial challenge for real-world generalization.

III. MATERIAL AND METHODS

A. Problem Statement

Tactile gesture recognition can be formulated as a multi-channel signal classification problem. When a human operator interacts with the robot using different gestures, the resulting sensor signals vary uniquely across joints, capturing distinct temporal and spatial patterns. These signals are typically high-dimensional, non-linear, and gesture-dependent in duration, making real-time classification challenging. Traditional rule-based or threshold-based methods struggle to handle such variability, necessitating the need for machine learning or deep learning approaches to effectively recognize and classify tactile gestures. This paper addresses three key research questions:

- How can a CNN-based algorithm be **designed** to recognize time-varying tactile gestures from internal robot sensors?
- What is the impact of different **input representations** (e.g., spectrograms vs. raw signals) on performance?
- How do the proposed models **perform**, and what factors explain performance differences?

B. Dataset Collection

Prior work has categorized human-to-robot touch gestures into different taxonomies, ranging from 30 [27] to as few as 4 [26]. In line with these studies, we define three key gestures (Single tap, Push, Grab) that sufficiently capture essential touch interactions for our demonstrator. *Single tap*

TABLE I: Proposed CNN-based models with their inputs, layer configurations, and key hyperparameters. (For Convolution Layer we only mentioned kernel size as padding are all 0 and stide are all 1)

Model Name	Model Details		
	Input	Layer Num.	Key Hyperparameters
STFT2DCNN	3D STFT Image	5	3DConv1(28 × 3 × 3) + 3DConv2(1 × 3 × 3) + 3D Pool(1 × 1 × 1) + Flatten + FC
STFT3DCNN	3D STFT Image	5	3DConv1(7 × 3 × 3) + 3DConv2(1 × 3 × 3) + 3D Pool(1 × 1 × 1) + Flatten + FC
STT2DCNN	3D STT Image	5	3DConv1(28 × 3 × 3) + 3DConv2(1 × 3 × 3) + 3D Pool(1 × 1 × 1) + Flatten + FC
STT3DCNN	3D STT Image	5	3DConv1(4 × 3 × 3) + 3DConv2(7 × 3 × 3) + 3D Pool(1 × 1 × 1) + Flatten + FC
RT2DCNN	3D RT Image	4	3DConv(28 × 3 × 3) + 3D Pool(1 × 1 × 1) + Flatten + FC
RT3DCNN	3D RT Image	5	3DConv1(5 × 3 × 3) + 3DConv2(5 × 3 × 3) + 3D Pool(1 × 1 × 1) + Flatten + FC

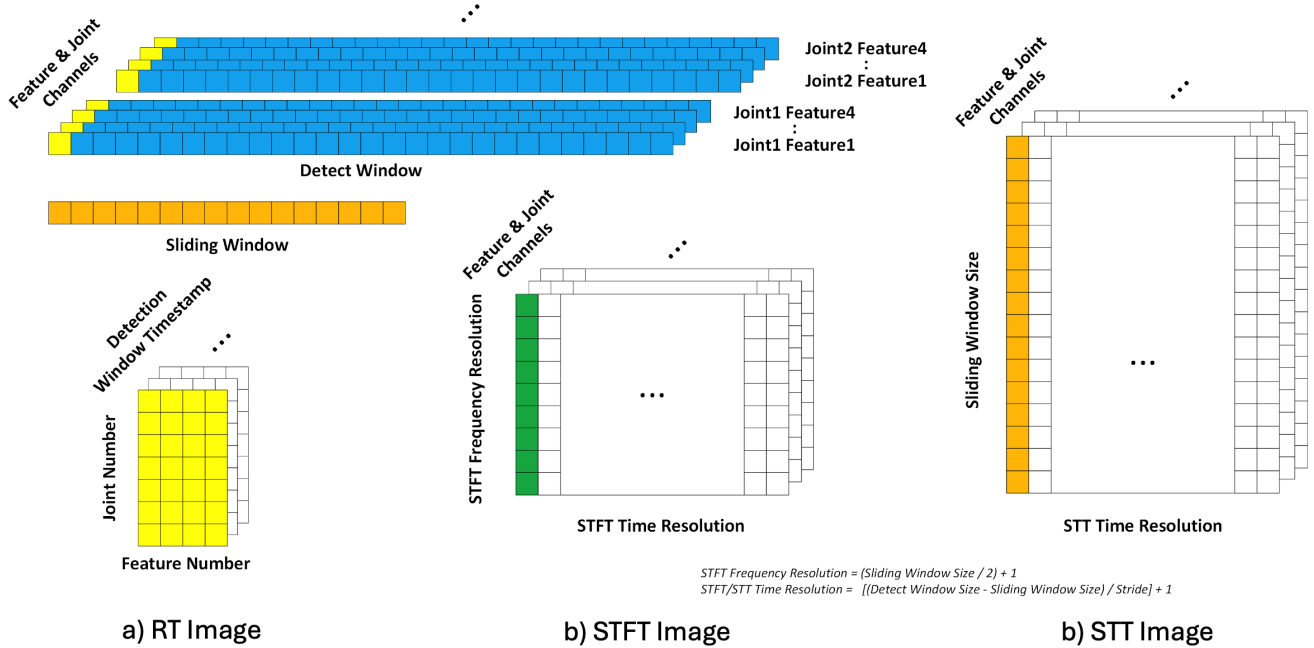


Fig. 1: The construction of all input format of our methods. Illustrate as parameter settings: Joint Number = 7, Feature Number = 4 ($e, \dot{e}, \tau, \tau_{ext}$), Detect Window Size = 28, Sliding Window Size = 16

is a brief, impulse-like touch applied to the robot surface without sustained pressure, such as pat, poke, or slap. **Push** is a sustained force applied to the robot with a clear direction, such as push, pull, or lift. **Grab** is a prolonged contact in which the hand encloses a link of the robot and applies stable pressure from multiple directions, such as pinch or squeeze.

Data were captured at a sampling frequency of 200 Hz using a digital glove and interacting with robot hand and the connected end effector in 5 directions (left, right, front, back, and up) and 10 positions. Data are segmented into fixed detection time windows of 28 timestamps with a step size of 14.

C. Gesture Recognition Models

We present models for real-time tactile gesture recognition on a Franka Emika robot, using only internal joint sensors. Various data representations are explored as model inputs.

1) *Traditional Machine Learning Methods*: According to Occam’s Razor [28], more complex models are not always superior. A simpler algorithm may, in some cases, outper-

form an elaborate deep learning model. As a baseline, we include a traditional K-Nearest Neighbor (KNN) classifier, a widely adopted method for classification tasks.

2) *CNN-Based Deep Learning Models*: Convolutional neural networks (CNNs) are effective in capturing temporal patterns in physical interaction data [12], [20], [23], [25]. Table I details the proposed architectures, which share the following structure:

- **Input Layer**: Receives one 3D image-like representations.
- **Convolutional Layers**: Learn spatial and temporal features via convolution filters.
- **Pooling Layer**: Reduces feature map dimensionality for computational efficiency and robustness.
- **Flatten Layer**: Converts 3D feature maps to 1D vectors.
- **Fully Connected Layer**: Outputs classification probabilities for each gesture.

3) *Input Data Representation*: For our gesture classification tasks, we leverage time-frequency analysis to handle the non-stationary nature of the sensor signals [29]. At each time

step t , the feature vector for joint, i is defined as

$$\mathbf{j}_t^i = \left[e_t^i, \dot{e}_t^i, \tau_t^i, \tau_t^{i,\text{ext}} \right],$$

where e_t^i is the joint position error, \dot{e}_t^i is the joint velocity error, τ_t^i is the measured joint torque, and $\tau_t^{i,\text{ext}}$ is the estimated external torque. We explore three distinct 3D data representations to serve as inputs for our models, each designed to test the significance of key signal properties:

- Whether frequency-domain features are necessary for accurate classification.
- Whether a pre-processing sliding-window operation is beneficial.

Non-Spectrogram (Raw-Time Stack): To serve as a baseline and investigate the impact of the sliding-window pre-processing itself, we construct a Raw-Time Stack. This representation is a 3D temporal structure formed by simply stacking the full time-series of joint-by-feature matrices, without any pre-processing windowing or transformation (Figure 1(a)).

Spectrogram: We generate spectrograms using the Short-Time Fourier Transform (STFT), a common time-frequency analysis technique for non-stationary signals [29]. We chose STFT over the more computationally demanding continuous wavelet transform to meet the real-time requirements of our system. To generate our spectrograms, we use a sliding-window operation on each feature and then apply the STFT. The resulting 2D spectrograms are stacked into a 3D structure with dimensions for frequency, time, and combined feature-joint indices, as illustrated in Figure 1(b).

Pseudo-Spectrogram: To specifically investigate whether frequency-based features are critical for performance, we introduce a Pseudo-Spectrogram (Figure 1(c)). This representation is constructed using the same sliding-window process as the STFT, thereby preserving the 3D input shape. However, it replaces the frequency-domain data with raw time-domain values. Comparing this representation with the Spectrogram will directly reveal the importance of frequency information.

4) *Majority Voting:* As noted by Czubenko et al. [23], filtering multiple consecutive detections can effectively reduce false positives. Therefore, for real-time deployment, we apply a majority-voting scheme over three consecutive detection windows for all our models, helping mitigate jitter in the classification results.

D. Hardware and Software Setup

The experimental platform consists of a Franka Emika Research collaborative robot, a digital glove with pressure sensors (Fig. 2), and a workstation for data processing and model training. The Franka Emika robot is a 7-degree-of-freedom (7-DoF) robotic arm equipped with joint-embedded torque sensors, used for tactile data collection and human-robot interaction experiments. The digital glove contains pressure sensors that detect contact events between humans and robots, transmitting real-time signals via the CANBUS protocol. The workstation, an HP Pro Mini 400 G9 Desktop

PC, is responsible for data processing and model training, featuring an Intel Core i7-13700T processor (16 cores, 24 threads, max 4.9 GHz clock speed) and 32 GB DDR4 3200 MHz memory.

The software environment is built on Ubuntu 20.04.6 LTS (Focal Fossa), providing a stable real-time computing framework for human-robot interaction experiments. The system uses Robot Operating System (ROS) as middleware for communication between software modules and the robot.

IV. EXPERIMENTAL RESULTS

A. Evaluation Metrics

To evaluate model performance, we follow the methodology in [30], assessing two aspects: (1) the ability to accurately detect contact events, and (2) the ability to correctly classify tactile gesture types.

1) *Contact Detection Metrics:* Since reliable contact detection is the basis for tactile gesture recognition, we quantify performance using the following metrics:

- **Accuracy (ACC, %):** Overall correctness in detecting contact events:

$$\text{ACC} = \frac{\text{TP} + \text{TN}}{\text{TP} + \text{TN} + \text{FP} + \text{FN}}. \quad (1)$$

- **Detection Failure Rate (DFR, %):** Proportion of actual contact events missed:

$$\text{DFR} = \frac{\text{FN}}{\text{TP} + \text{FN}}. \quad (2)$$

- **False Alarm Rate (FAR, %):** Proportion of incorrect contact detections:

$$\text{FAR} = \frac{\text{FP}}{\text{TN} + \text{FP}}. \quad (3)$$

- **Detection Delay (DD, ms):** The time required for the model to recognize a contact occurrence.
- **Recovery Delay (RD, ms):** The time required for the model to recognize the end of a contact event.

As noted in [30], lower DFR and FAR indicate a more robust detector. Delays exceeding 150 ms in either DD or RD are treated as misclassifications.

2) *Gesture Classification Metrics:* Gesture classification performance is assessed only within correctly detected contact regions (True Positive segments in Fig. 3) to avoid bias from detection errors. We report the following metrics:

- **Accuracy (ACC, %):** Measures the overall correctness in classifying gesture types, defined as:

$$\text{ACC} = \frac{\text{TP}_{\text{gesture}}}{\text{TP}_{\text{contact}}}. \quad (4)$$

- **Per-gesture Detection Failure Rate (%):** Contact localization failure rate for individual gesture defined as Eq 2.

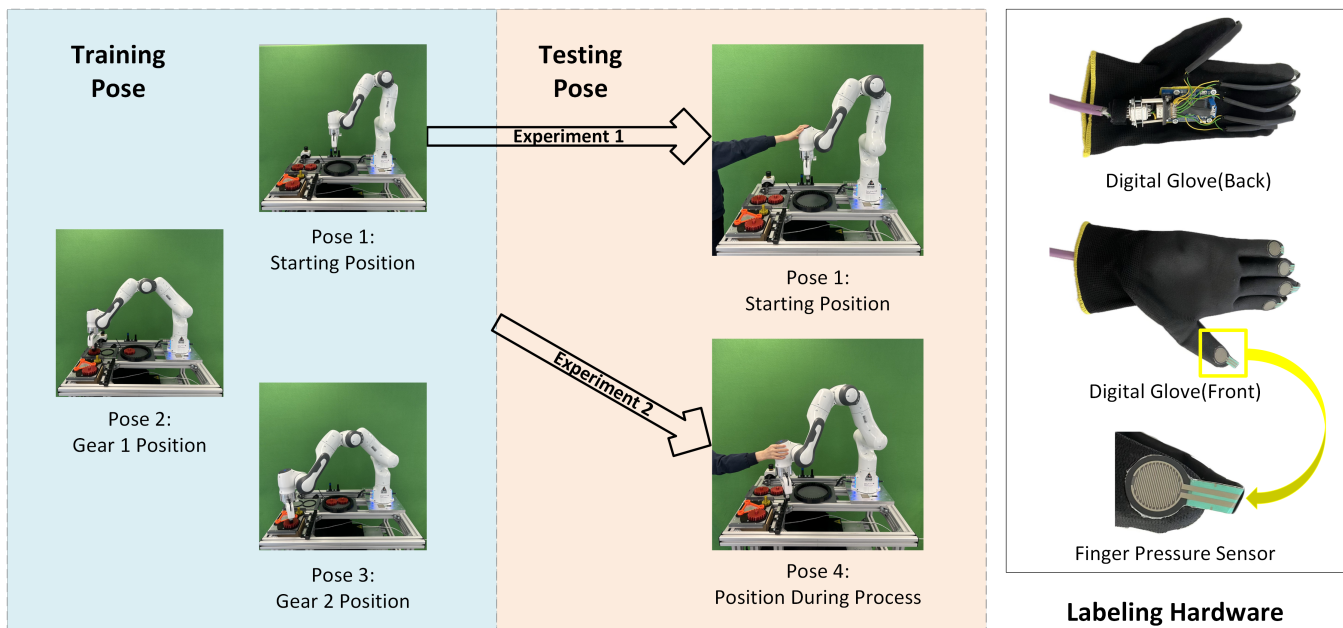


Fig. 2: Experimental Setup (Gear Assembling Task): Left part shows 3 poses in the assembling procedure that used to collect training data; Middle part shows 2 test poses used in experiment 1 and 2; Right part shows the digital glove and its pressure sensor

TABLE II: Performance comparison of different models based on Contact Detection and Touch Classification Metrics . ($RD = 0$ doesn't mean there is no recovery delay, but as the delay exceeds our threshold(150 ms), they will all be marked as FP)

Eperiment	Models	Contact Detection Metrics					Gesture Classification Metrics			
		Acc. (%)	DFR (%)	FAR (%)	DD (ms)	RD (ms)	Acc. (%)	DFR (%)		
								ST	P	G
EXP1	STFT2DCNN	95.98	3.01	3.65	45.12	75.00	95.72	1.35	9.12	2.37
	STFT3DCNN	94.42	0.84	6.17	57.80	72.50	93.05	0	14.37	6.47
	STT2DCNN	96.42	0.47	4.39	64.64	0	88.76	25.00	6.49	1.78
	STT3DCNN	94.69	0.13	6.22	61.83	75.00	94.26	3.23	7.49	6.50
	RT2DCNN	96.92	4.36	2.22	68.20	53.74	92.36	5.31	11.86	5.74
	RT3DCNN	96.12	0.81	4.30	61.00	81.66	91.58	9.52	8.77	6.95
EXP2	STFT2DCNN	95.64	2.04	4.57	47.61	70.00	95.76	3.85	7.77	1.11
	STFT3DCNN	96.22	1.64	4.15	51.45	56.67	93.08	1.27	10.30	9.18
	STT2DCNN	95.81	1.26	4.43	52.12	39.99	92.25	8.16	10.14	4.95
	STT3DCNN	95.62	1.02	4.95	51.48	85.00	95.92	2.78	7.81	1.65
	RT2DCNN	93.85	1.96	6.94	61.41	75.00	71.17	36.73	8.07	41.67
	RT3DCNN	92.59	0.19	8.39	51.89	32.51	71.67	45.83	4.23	34.93

B. EXP1: Gesture Detection in a Known Robot Pose

This experiment evaluates the models' ability to classify gesture types in a fixed robot pose (Pose 1, Fig. 2). Training and testing are conducted on the same pose to assess accuracy in distinguishing gestures. The KNN baseline was excluded after preliminary testing, as it failed to reliably separate gestures from one another or from no-contact cases. In addition, increasing training data caused cumulative delays that violated real-time constraints. Final results are presented in Table II. STFT2DCNN and STT3DCNN models achieve the highest gesture classification accuracy while maintaining competitive contact detection performance.

C. EXP2: Cross-Pose Generalization

This experiment evaluates generalization to unseen robot poses (Fig. 2). Models are trained on data from Poses 1–3 and tested on Pose 4, introducing a distribution shift. Results in Table II show that spectrogram-based models generalize significantly better than non-spectrogram approaches. Compared with EXP1, the reduction in contact detection and gesture classification accuracy is minimal—and in some cases, accuracy improves. This indicates that frequency-domain features captured by spectrograms are more robust to pose variation. This shows that features captured by constructing spectrogram or pseudo-spectrogram representations yield

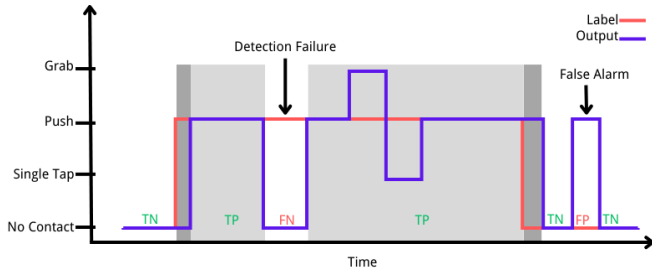


Fig. 3: Evaluation Example: A Single Push. True Negative (TN): The model correctly identifies no contact when there is no contact. True Positive (TP): The model correctly detects a contact event when contact occurs. False Negative (FN): The model fails to detect contact when contact actually occurs. False Positive (FP): The model falsely detects contact when no contact occurs.

TABLE III: Contact Detection (CD) and Gesture Classification (GC) performance comparison of 2D and 3D CNNs with different convolutional structures. In “Conv. Structures”, notation $x + y$ denotes that the kernel size in the third dimension (the combined feature-joint indices dimension, as shown in Fig. 1) is set to x in the first convolutional layer and y in the second convolutional layer.

Models	Conv. Structures	CD Acc. (%)	GC Acc. (%)
STFT2DCNN	28+1	95.64	95.76
STFT3DCNN	7+1	96.22	93.08
	4+7	-	-
STT2DCNN	28+1	95.81	92.25
STT3DCNN	7+1	92.50	86.05
	4+7	95.62	95.92

models that are more robust to pose variation. For example, STFT3DCNN’s contact detection accuracy increases from 94.42% to 96.22%, while its gesture classification accuracy rises slightly from 93.05% to 93.08%.

D. EXP3: Impact of 3D Convolutions and Frequency Transformations

This experiment investigates whether 3D convolutions and frequency-domain transformations (e.g., STFT) influence performance. We compare STFT2DCNN and STT2DCNN (2D CNNs) with STFT3DCNN and STT3DCNN (3D CNNs) using identical network architectures.

The STFT3DCNN and STT3DCNN results in Tables II correspond to **STFT3DCNN7+1** and **STT3DCNN4+7**, respectively. From Table III, we find that **under identical architecture**, introducing **3D convolution** can reduce gesture classification accuracy (e.g., STFT/STT2DCNN vs. STFT/STT3DCNN7+1). However, slightly deepening the 3D CNN (STT3DCNN7+1 \rightarrow STT3DCNN4+7) improves performance, even surpassing STT2DCNN in Experiment 2.

Increasing STFT3DCNN complexity (STFT3DCNN7+1 \rightarrow STFT3DCNN4+7) introduces substantial cumulative delay, which prevented evaluation of accuracy and is therefore indicated as “-” in the table. This delay disappears on

a high-performance GPU workstation, indicating that real-time viability depends strongly on available hardware. In conclusion, both frequency transformations (STT \rightarrow STFT) and 3D convolutions incur extra computation and have a relatively substantial impact on model performance.

V. DISCUSSION

A. Result Analysis and Answering Research Questions

RQ1: Our experiments validate the design of a CNN-based framework for tactile gesture recognition. The high performance of our leading models, such as STFT2DCNN and STT3DCNN, with over 95% accuracy in contact detection and gesture classification, demonstrates the effectiveness of our design.

RQ2: Our results clearly demonstrate that spectrogram-based methods significantly outperform non-spectrogram methods in tactile gesture recognition. This indicates that constructing spectrogram or pseudo-spectrogram representations — through sliding-window segmentation and column-wise stacking — is highly beneficial when combined with CNN architectures. However, for simpler tasks like only contact detection, less complex non-spectrogram methods are sufficient.

RQ3: To understand the factors contributing to these results, we compared CNNs with different architectures. Our findings show that applying 3D convolutions can sometimes decrease gesture classification performance under identical network structures. However, a slightly deeper 3D CNN architecture can improve accuracy, sometimes surpassing the 2D CNNs. Both frequency transformations (like STFT) and 3D convolutions introduce additional computational costs. This highlights a key trade-off between model complexity, task demands, and available computational resources. Therefore, **the decision to use them should be task-dependent:**

- For complex gesture recognition tasks requiring higher accuracy, well-chosen spectrogram-based representations and carefully designed 3D CNNs may be justified.
- For simpler tasks or systems with limited computational capacity, **2D CNNs combined with STFT**, or **3D CNNs without frequency transformations**, already offer an effective trade-off between accuracy and efficiency.

In summary, **system designers should carefully balance model complexity, task demands, and available computational resources** when designing tactile gesture recognition systems.

B. Limitations and Outlook

Our experiments were conducted under specific robot poses (Pose 1, 2, 3 for training and Pose 4 for testing), designed based on our gear-assembling task. This constrained experimental setup limits the pose generalization ability of the proposed models. In real-world applications, robots are expected to handle tactile gestures under a wider variety of poses. Although we evaluated cross-pose generalization to some extent (by testing on unseen Pose 4), the performance under poses that significantly deviate from the training trajectory remains unknown and could degrade. Moreover,

contact location generalization is also a concern. All gestures were applied solely to link 7 and the end-effector as required by the task. Consequently, our models may have implicitly overfitted to these specific robot parts, potentially leading to poor performance if tactile gestures are applied to other parts of the robot. Additionally, all experiments were conducted on a single robotic platform — the Franka Emika Research. While representative, the model’s transferability to other cobots, such as the UR series, has not been evaluated. Since hardware characteristics (e.g., joint sensor precision, dynamic response) vary, this is a crucial limitation for broader industrial deployment.

Although the total amount of training data is considerable, our dataset still suffers from imbalances and coverage limitations. In Experiment 1 (Ex1), which used only Pose 1 for training, the number of complete gesture instances (ST, P, G) was limited across the 10 positions. As a result, some models may exhibit “blind spots” in recognizing gestures performed at underrepresented positions. This issue was partially alleviated in Experiment 2 (Ex2), where combining training data from three poses (Pose 1, 2, and 3) increased the diversity of gesture samples. This improvement correlates with the significant performance gains observed in models like ST2DCNN, whose accuracy notably improved from Ex1 to Ex2. This highlights the importance of gesture variability and pose diversity in training data for robust tactile recognition.

Our proposed methods focus exclusively on CNN-based architectures, without exploring more recent alternatives such as Transformer-based models. While Transformers have shown strong performance in various sequence modeling tasks, their application to tactile signals could offer advantages in capturing complex spatiotemporal patterns. However, such models typically require very large datasets. Exploring Transformer-based or hybrid architectures is a promising direction for future work that could lead to improved accuracy, better generalization, or swifter response.

REFERENCES

- [1] X. Xu, Y. Lu, B. Vogel-Heuser, and L. Wang, “Industry 4.0 and industry 5.0— inception, conception and perception,” *Journal of Manufacturing Systems*, vol. 61, pp. 530–535, 2021. [Online]. Available: <https://www.sciencedirect.com/science/article/pii/S0278612521002119>
- [2] P. K. R. Maddikunta, Q.-V. Pham, P. B. N. Deepa, K. Dev, T. R. Gadekallu, R. Ruby, and M. Liyanage, “Industry 5.0: A survey on enabling technologies and potential applications,” *Journal of Industrial Information Integration*, vol. 26, p. 100257, 2022. [Online]. Available: <https://www.sciencedirect.com/science/article/pii/S2452414X21000558>
- [3] J. Leng, W. Sha, B. Wang, P. Zheng, C. Zhuang, Q. Liu, T. Wuest, D. Mourtzis, and L. Wang, “Industry 5.0: Prospect and retrospect,” *Journal of Manufacturing Systems*, vol. 65, pp. 279–295, 2022. [Online]. Available: <https://www.sciencedirect.com/science/article/pii/S0278612522001662>
- [4] M. Rubagotti, I. Tusseyeva, S. Baltabayeva, D. Summers, and A. Sandygulova, “Perceived safety in physical human–robot interaction—a survey,” *Robotics and Autonomous Systems*, vol. 151, p. 104047, 2022.
- [5] C. Pohlt, F. Haubner, J. Lang, S. Rochholz, T. Schlegl, and S. Wachsmuth, “Effects on user experience during human-robot collaboration in industrial scenarios,” in *2018 IEEE International Conference on Systems, Man, and Cybernetics (SMC)*. IEEE, 2018, pp. 837–842.
- [6] Z. Hu, L. Lin, W. Lin, Y. Xu, X. Xia, Z. Peng, Z. Sun, and Z. Wang, “Machine learning for tactile perception: Advancements, challenges, and opportunities,” *Advanced Intelligent Systems*, vol. 5, no. 7, p. 2200371, 2023. [Online]. Available: <https://advanced.onlinelibrary.wiley.com/doi/abs/10.1002/aisy.202200371>
- [7] J. A. Barreiros, A. Xu, S. Pugach, N. Iyengar, G. Troxell, A. Cornwell, S. Hong, B. Selman, and R. F. Shepherd, “Haptic perception using optoelectronic robotic flesh for embodied artificially intelligent agents,” *Science Robotics*, vol. 7, no. 67, p. eabi6745, June 2022.
- [8] F. Liu, S. Deswal, A. Christou, Y. Sandamirskaya, M. Kaboli, and R. Dahiya, “Neuro-inspired electronic skin for robots,” *Science Robotics*, vol. 7, no. 67, p. eabl7344, 2022. [Online]. Available: <https://www.science.org/doi/abs/10.1126/scirobotics.abl7344>
- [9] W. Wang, Y. Jiang, D. Zhong *et al.*, “Neuromorphic sensorimotor loop embodied by monolithically integrated, low-voltage, soft e-skin,” *Science*, vol. 380, no. 6646, pp. 735–742, 2023.
- [10] B. Shih, D. Shah, J. Li *et al.*, “Electronic skins and machine learning for intelligent soft robots,” *Science Robotics*, vol. 5, no. 41, p. eaaz9239, 2020.
- [11] Z. Huang, S. Yu, Y. Xu *et al.*, “In-sensor tactile fusion and logic for accurate intention recognition,” *Advanced Materials*, vol. 36, no. 35, p. e2407329, 2024.
- [12] Y. J. Heo, D. Kim, W. Lee, H. Kim, J. Park, and W. K. Chung, “Collision detection for industrial collaborative robots: A deep learning approach,” *IEEE Robotics and Automation Letters*, vol. 4, no. 2, pp. 740–746, 2019.
- [13] S. D. Lee and J. B. Song, “Sensorless collision detection based on friction model for a robot manipulator,” *International Journal of Precision Engineering and Manufacturing*, vol. 17, no. 1, pp. 11–17, January 2016.
- [14] S. El Zaatari, M. Marei, W. Li, and Z. Usman, “Cobot programming for collaborative industrial tasks: An overview,” *Robotics and Autonomous Systems*, vol. 116, pp. 162–180, 2019. [Online]. Available: <https://www.sciencedirect.com/science/article/pii/S092188901830602X>
- [15] C. Zech, J. Römhild, P. Gsellmann, M. Melik-Merkumians, and G. Schitter, “Sensorless external torque sensing for collision detection in collaborative robots,” in *IECON 2023- 49th Annual Conference of the IEEE Industrial Electronics Society*, 2023, pp. 1–6.
- [16] T. Ren, Y. Dong, D. Wu, and K. Chen, “Collision detection and identification for robot manipulators based on extended state observer,” *Control Engineering Practice*, vol. 79, pp. 144–153, 2018. [Online]. Available: <https://www.sciencedirect.com/science/article/pii/S0967066118302466>
- [17] D. Zurlo, T. Heitmann, M. Morlock, and A. D. Luca, “Collision detection and contact point estimation using virtual joint torque sensing applied to a cobot,” in *2023 IEEE International Conference on Robotics and Automation (ICRA)*, London, United Kingdom, 2023, pp. 7533–7539.
- [18] A.-N. Sharkawy, P. N. Koustoumpardis, and N. Aspragathos, “Human–robot collisions detection for safe human–robot interaction using one multi-input–output neural network,” *Soft Computing*, vol. 24, no. 9, pp. 6687–6719, Aug 2019.
- [19] A.-N. Sharkawy and A. A. Mostfa, “Neural networks design and training for safe human-robot cooperation,” *Journal of King Saud University - Engineering Sciences*, vol. 34, no. 8, pp. 582–596, 2022. [Online]. Available: <https://www.sciencedirect.com/science/article/pii/S1018363921000209>
- [20] K. M. Park, J. Kim, J. Park, and F. C. Park, “Learning-based real-time detection of robot collisions without joint torque sensors,” *IEEE Robotics and Automation Letters*, vol. 6, no. 1, pp. 103–110, Jan 2021.
- [21] K. M. Park, Y. Park, S. Yoon, and F. C. Park, “Collision detection for robot manipulators using unsupervised anomaly detection algorithms,” *IEEE/ASME Transactions on Mechatronics*, vol. 27, no. 5, pp. 2841–2851, Oct 2022.
- [22] F. Min, G. Wang, and N. Liu, “Collision detection and identification on robot manipulators based on vibration analysis,” *Sensors*, vol. 19, no. 5, p. 1080, Mar 2019. [Online]. Available: <https://doi.org/10.3390/s19051080>
- [23] M. Czubenko and Z. Kowalczyk, “A simple neural network for collision detection of collaborative robots,” *Sensors*, vol. 21, no. 12, p. 4235, 2021. [Online]. Available: <https://doi.org/10.3390/s21124235>
- [24] D. Kim, D. Lim, and J. Park, “Transferable collision detection learning for collaborative manipulator using versatile modularized neural net-

- work,” *IEEE Transactions on Robotics*, vol. 38, no. 4, pp. 2426–2445, 2022.
- [25] F. M. Amin, M. Rezayati, H. W. van de Venn, and H. Karimpour, “A mixed-perception approach for safe human-robot collaboration in industrial automation,” *Sensors*, vol. 20, no. 21, p. 6347, 2020. [Online]. Available: <https://doi.org/10.3390/s20216347>
- [26] B. Bianchini, P. Verma, and J. K. Salisbury, “Towards human haptic gesture interpretation for robotic systems,” in *2021 IEEE/RSJ International Conference on Intelligent Robots and Systems (IROS)*. IEEE Press, 2021, p. 7334–7341. [Online]. Available: <https://doi.org/10.1109/IROS51168.2021.9636015>
- [27] S. Yohanan and K. E. MacLean, “The role of affective touch in human-robot interaction: Human intent and expectations in touching the haptic creature,” *International Journal of Social Robotics*, vol. 4, pp. 163–180, 2012. [Online]. Available: <https://doi.org/10.1007/s12369-011-0126-7>
- [28] A. Blumer, A. Ehrenfeucht, D. Haussler, and M. K. Warmuth, “Occam’s razor,” *Information Processing Letters*, vol. 24, no. 6, pp. 377–380, 1987. [Online]. Available: <https://www.sciencedirect.com/science/article/pii/0020019087901141>
- [29] Y. Yang, Z. Peng, W. Zhang, and G. Meng, “Parameterised time-frequency analysis methods and their engineering applications: A review of recent advances,” *Mechanical Systems and Signal Processing*, vol. 119, pp. 182–221, 2019. [Online]. Available: <https://www.sciencedirect.com/science/article/pii/S088832701830445X>
- [30] M. Rezayati, K. M. Park, and H. W. van de Venn, “Learning-based contact interpretation with lstm networks: A transferable skill for robots,” *TechRxiv*, May 2025. [Online]. Available: <https://doi.org/10.36227/techrxiv.174742058.83011810/v1>